PERGAMON

Available online at www.sciencedirect.com
SCIENCE DIRECT®

International Journal of Heat and Mass Transfer 46 (2003) 2095–2101

International Journal of HEAT and MASS TRANSFER

www.elsevier.com/locate/ijhmt

Study on transport phenomena for flow film condensation in vertical mini-tube with interfacial waves

Xiao-Ze Du [a], Bu-Xuan Wang [b,*]

[a] Department of Thermal Power Engineering, North China Electric Power University, Beijing 102206, China
[b] Department of Thermal Engineering, Tsinghua University, Beijing 100084, China

Received 9 September 2002

Abstract

The Kelvin–Helmholtz instability of phase-change interface during flow film condensation in vertical mini-diameter tube was studied here by means of energy analysis. According to the interfacial boundary conditions, the film thinning effect and the phase-change area enlarging effect by interfacial waves on heat transfer enhancement were analyzed for flow condensation in tubes with different diameter. It is indicated that, in mini-diameter tube, more obvious heat transfer enhancement due to interfacial waves can be expected than that in normal-sized tube, and the interfacial waves enhance the heat transfer mainly by film thinning effect.

Keywords: Flow film condensation; Vertical mini tube; Kelvin–Helmholtz instability; Energy analysis

1. Introduction

Much more works have been done concerning laminar film flow condensation in commercial tubes since the earliest and classical work of Nusselt [1]. The revised Nusselt models to take care the factors neglected by Nusselt, such as variable wall surface temperature and interfacial transport phenomena, have been examined in more consistent base, and are remarkably successful to predict the relevant parameters in most traditional industrial fields [2]. As concluded by Incropera and Dewitt [3], the heat transfer enhancement of condensation affected by phase-change interfacial waves is not more than 20% if the shear stress between liquid and vapor phase can be neglected, and the interfacial waves affect only when $Re_l > 20$–30. However, the development of technology needs more compact and efficient heat exchangers in many applications, where the tube diameter of heat exchangers is reduced to less than 3–5 mm, named as mini-tube, such as for the automotive air conditioners or life-support systems in space, and also, the recent advances for the development of micromechanical systems. Rohsenow [4] had declared early in 1970 that, in such mini-tubes, the bending effect of condensate film cannot be neglected, which void the "plate" approximations in Nusselt theory. Our previous works [5–7] to study the flow condensation along small/mini-diameter tube also indicate that the effect of surface tension on condensation can no longer be neglected and the shear stress on liquid–vapor interface has more important effect than gravity, even at small Reynolds number. Surely, the increasing effect of shear stress and surface tension will bring more obvious perturbation on condensate film, and accordingly, will enhance the film instability. It is therefore logical to deduce that the interfacial waves may have more obvious effect on heat transfer in mini-tube than that in ordinary sized tube. It is the purpose of present work to investigate the behavior of interfacial wave and its influences on heat transfer during flow film condensation in mini-tube.

According to Ramkrishna and Pattanayak [8], the present paper assumes the amplitudes of the waves growing due to the Kelvin–Helmholtz instability. Occurrence of finite amplitude capillary waves is responsible

* Corresponding author. Tel.: +86-10-6278-4526; fax: +86-10-6277-0209.
E-mail address: bxwang@mail.tsinghua.edu.cn (B.-X. Wang).

0017-9310/03/$ - see front matter
doi:10.1016/S0017-9310(02)00469-6

Nomenclature

A	cross-sectional area, m^2
c_f	friction factor
E	energy per unit area in displacing wave crest, J/m^2
F	force per unit area, N/m^2
g	gravitational acceleration, m/s^2
h_{lv}	latent heat, J/kg
I_0	Bessel function
k	thermal conductivity of condensate film, W/m °C
$\dot{m}_l$	liquid flux, kg/s
Nu	Nusselt number, dimensionless
p	pressure, Pa
Pr	Prandtl number, dimensionless
r	radius, or co-ordinate in radial direction, m
R	radius of tube, m
Re	Reynolds number, dimensionless
T	temperature, °C
u	velocity, m/s
x	quality, dimensionless
y	distance from tube wall, m
z	co-ordinate in axial direction, m
z_0	the intersecting position of interfacial waves and tube wall, m

Greek symbols

α	heat transfer coefficient, W/m^2 °C
β	the angle between wavy interface and tube wall
δ	the film thickness, m
λ	wavelength, m
μ	viscosity, kg/m s
ρ	density, kg/m^3
τ_s	surface tension, N/m
τ_δ	shear stress on interface, N/m^2
ζ	amplitude of wave, m

Superscript

–	average value

Subscripts

0	initial value
B	Bernoulli effect
E	perturbation wavelength
l	liquid
lv	vapor–liquid interface
lw	solid–liquid interface
s	surface or saturation
sat	saturation
v	vapor
w	tube wall
wave	waving interface

for such an appearance. The wavy interface and the interfacial boundary conditions are treated by work or energy analysis, based on which, the effects of interfacial capillary waves on heat transfer characteristics of flow film condensation in mini-tubes are analyzed.

2. Analysis on interfacial waving

The physical model for saturated vapor flowing at temperature of T_{sat} and condensed on the cooled inside wall surface of a vertical mini-tube, to form a condensate film is shown in Fig. 1. The film was affected jointly by gravity, shear stress on surfaces and surface tension due to condensate film bending.

According to Kelvin–Helmholtz instability theory, the amplitude of the waves can be promoted by the suction force at the wave crest, developed as a result of the Bernoulli effect. In addition, the capillary force caused by film bending in axial direction can also enhance the waving. The capillary force caused by film bending in radial direction will restrain the interface waving. While the waves spread to the tube wall, the enhancement of condensed film instability will be restricted accordingly by capillary adhesion force between the wall and the fluid. Thus, the interfacial waving behaviors should be established by the equilibrium of these forces.

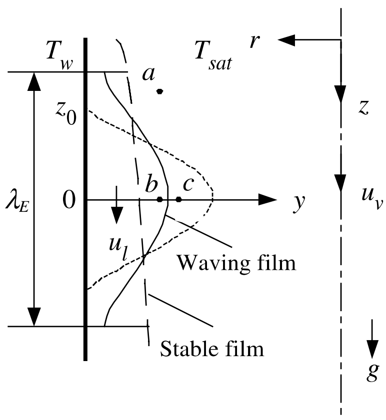

Fig. 1. Physical model.

Assume: (a) The interfacial waves grow from the stable state of zero amplitude such that the cross-sectional area parallel to the axis of the liquid film under the wave profile, A_{wave}, remains constant during the growth of the waves. (b) The pressure drop from the base to the top of the liquid lump is small enough to be neglected. (c) The axially symmetric wave profile can be expressed as cosine function, $y(z) = \delta = \delta_s + \zeta\cos((2\pi/\lambda)z)$, where δ_s is the stable film thickness, ζ and λ are the amplitude and wavelength. (d) The film thickness δ_s is thought to be constant in range of wavelength.

As the wave grows with a constant average cross-sectional area, the radius of curvature at the crest becomes smaller, and the capillary force caused by film bending in radial direction increases gradually. The Bernoulli suction force also increases due to the narrowing of gas flow passage. Then, the work generated or energy involved, $E(y)$, by the capillary force, F_s, Bernoulli force, F_B, and also, the possible adhesion force on tube wall, F_w, in displacing the wave crest, can be obtained as

$$E(y) = \int_0^{y-\delta} [F_B(\zeta) - F_s(\zeta)]\,d\zeta, \quad \text{for } \zeta < \delta \quad \text{and} \quad \delta \leqslant y \leqslant 2\delta \tag{1a}$$

$$E(y) = \int_0^{y-\delta} [F_B(\zeta) - F_s(\zeta)]\,d\zeta - 2\int_\delta^{y-\delta} F_w(\zeta)\,dz_0, \quad \text{for } \zeta > \delta \quad \text{and} \quad 2\delta \leqslant y \leqslant R \tag{1b}$$

among which z_0 is the intersecting position of interfacial waves and tube wall. Refer to Fig. 1, $y(z) = \delta_s + \zeta\cos((2\pi/\lambda)z)$ approximates to 0 at $z = z_0$ if $\zeta > \delta_s$. For such a case, the condensate film would break and the phenomenon of "liquid bridge" might be developed. z_0 is thereby given as

$$z_0 = \frac{\lambda}{2\pi}\cos^{-1}\left(-\frac{\delta_s}{\zeta}\right) \tag{2}$$

where $\lambda = \lambda_E$, $A_{wave} = \delta\lambda_E$ for $\zeta \leqslant \delta_s$; or $A_{wave} = \int_{-z_0}^{z_0} y(z)\,dz$ for $\zeta > \delta_s$, then,

$$\lambda = A_{wave} \Bigg/ \left\{ \frac{\delta_s}{\pi}\cos^{-1}\left(-\frac{\delta_s}{\zeta}\right) + \frac{\zeta}{\pi}\sin\left[\cos^{-1}\left(-\frac{\delta_s}{\zeta}\right)\right]\right\} \tag{3}$$

So, z_0 can be expressed as a function of ζ. Differentiating z_0 with respect to ζ, we obtain

$$dz_0 = \left[\frac{1}{2\pi}\frac{d\lambda}{d\zeta}\cos^{-1}\left(-\frac{\delta_s}{\zeta}\right) + \frac{\lambda}{2\pi}\frac{-1}{\sqrt{1-\delta^2/\zeta^2}}\left(\frac{\delta_s}{\zeta^2}\right)\right]d\zeta \tag{4}$$

in which $d\lambda/d\zeta$ can be determined from differentiating Eq. (3).

As long as the total energy provided by suction force is greater than that required for working against capillary forces, $E(y)$ remains positive so that the wave crest will continue to grow up, which indicates that the system has enough energy to enhance the film instability. However, as $E(y) < 0$, the crest starts reverting and the system does not acquire the ability to maintain interface waving increasingly. So, $E(y) = 0$ means the minimum energy state of the system and the most possible state of the waving interface as there is no more residual energy in displacing wave crest.

The parameters in Eqs. (1a) and (1b) are calculated as follows:

Because the wavelength is much smaller than the tube length, the pressure drop within the respect of order of wavelength can be neglected, i.e. $p_a = p_b$ in Fig. 1. According to assumption (b), p_b is equal to the wave crest pressure, we can thus induce from Bernoulli equation:

$$F_B(\zeta) = p_b - p_c = \frac{\rho_v}{2}(\bar{u}_v - \bar{u}_l)^2\left[\left(\frac{R-\delta_s}{R-\delta_s-\zeta}\right)^4 - 1\right], \tag{5}$$

where $\bar{u}_v$ and $\bar{u}_l$ are the average velocity of liquid and vapor phases respectively.

By the well-known Young–Laplace equation, we have the interfacial force on condensate film surface as

$$F_s(\zeta) = -\sigma_{lv}\left(\frac{1}{r_{lv,1}} + \frac{1}{r_{lv,2}}\right) \tag{6}$$

with

$$\frac{1}{r_{lv,1}} = \frac{1}{R-\delta_s-\zeta}, \quad \frac{1}{r_{lv,2}} = \frac{y''}{(1+y'^2)^{3/2}}\bigg|_{z=0} = -\zeta\frac{4\pi^2}{\lambda^2}$$

and the adhesion force on the wall surface as

$$F_w(\zeta) = -\sigma_{lv}\cos\beta\left(\frac{1}{r_{lw,1}} + \frac{1}{r_{lw,2}}\right) \tag{7}$$

where β is the angle between wavy interface and tube wall, i.e. $tg\beta = y'|_{z=z_0}$, $1/r_{lw,1} = 1/R$, $1/r_{lw,2} = y''(1+y'^2)^{3/2}|_{z=z_0}$; y is the position of waving interface as shown in Fig. 1.

The condensate film thickness, δ_s, and average velocity of liquid and vapor phases, $\bar{u}_v$ and $\bar{u}_l$ are predicted by the following model of flow condensation with smooth vapor–liquid interface.

3. Modeling of flow condensation in vertical mini-tube

3.1. Mathematical model

For the typical case $\zeta \to 0$, $\delta \to \delta_s$, the inertia term in momentum equation and convective term in energy equation of liquid phase are both negligible-, we can express the mathematical model of flow condensation in vertical mini-tube as:

3.1.1. Momentum equation of condensate film

$$\frac{1}{r}\frac{\partial}{\partial r}\left(r\mu\frac{\partial u_l}{\partial r}\right)-\frac{dP_l}{dz}+\rho_l g=0 \tag{8}$$

with boundary conditions: $r=R$, $u_l=0$;

$$r=R-\delta,\quad -\mu\frac{\partial u_l}{\partial r}=\tau_\delta \tag{9}$$

τ_δ denotes the shear stress on vapor–liquid interface.

3.1.2. Energy equation of condensed film

$$\frac{2\pi\lambda(T_s-T_w)}{\ln(R/(R-\delta))}=\frac{d\dot{m}_{lz}}{dz}h_{lv} \tag{10}$$

where $\dot{m}_{lz}$ is the liquid flux at z, and h_{lv} is the latent heat of vapor.

3.1.3. Continuity equation

$$\dot{m}_{lz}+\dot{m}_{vz}=\dot{m}_{v0} \tag{11}$$

3.2. Solution of the model

3.2.1. Velocity field in liquid film

Combined Eq. (8) and the boundary conditions, Eq. (9), yields:

$$u_l=\frac{1}{2\mu}\left(\frac{dp_l}{dz}-\rho_l g\right)\left[\frac{r^2-R^2}{2}-(R-\delta)^2\ln\frac{r}{R}\right]-\frac{\tau_\delta(R-\delta)}{\mu}\ln\frac{r}{R} \tag{12}$$

3.2.2. Mass flux of liquid film

$$\dot{m}_{lz}=\int_{R-\delta}^{R}2\pi r\rho_l u_l\,dr \tag{13}$$

From energy equation of condensate film, we can obtain another expression of mass flux:

$$\dot{m}_{lz}=\frac{1}{h_{lv}}\int_0^z\frac{2\pi\lambda(T_s-T_w)}{\ln(R/R-\delta)}\,dz \tag{14}$$

3.2.3. Average velocity of vapor flow

$$\overline{u_{zv}}=(\pi R^2\rho_v u_{v0}-\dot{m}_{zzl})/[\pi(R-\delta)\rho_v]=\frac{R^2}{(R-\delta)^2}u_{v0}-\frac{\dot{m}_{lz}}{\pi(R-\delta)^2\rho_v} \tag{15}$$

3.2.4. Pressure drop

$$\frac{dp_v}{dz}=\rho_v g-\frac{2\tau_\delta}{R-\delta} \tag{16}$$

In small/mini-diameter tube, the bend of liquid film along axial direction cannot be neglected [4]. A force balance for the curved vapor–liquid interface gives,

$$p_v-p_l=\frac{\sigma_{lv}}{R-\delta} \tag{17}$$

Differentiating with Eq. (17) respect to z, yields the pressure drop of liquid film as

$$\frac{dp_l}{dz}=\rho_v g-\frac{2\tau_\delta}{(R-\delta)}+\frac{\sigma_{lv}}{(R-\delta)^2}\frac{d(R-\delta)}{dz} \tag{18}$$

3.2.5. Shear stress on vapor–liquid interface τ_δ

$$\tau_\delta=\pm\frac{c_f}{2}\rho_v(\overline{\boldsymbol{u}_{vz}}-\boldsymbol{u}_{lz})^2+\frac{1}{2\pi(R-\delta)}\frac{d\dot{m}_{lz}}{dz}(\overline{\boldsymbol{u}_{vz}}-\boldsymbol{u}_{lv}) \tag{19}$$

where the calculation of friction factor c_f can refer to [9].

Eqs. (12)–(19) can be solved numerically. At a given axial location, z, the film thickness δ_s is calculated, and in turn, the values of system quality, x, liquid Reynolds number, Re_l, and average velocity of condensate film, $\bar{u}_l$, are calculated as:

$$x=\frac{m_{v0}-m_{lz}}{m_{v0}},\quad Re_l=\frac{4m_{lz}}{\mu_l\pi D},\quad \bar{u}_l=\frac{m_{lz}}{\rho_l\pi[R^2-(R-\delta)^2]}.$$

With smooth vapor–liquid interface, the Nusselt number of condensation heat transfer at every step is obtained by

$$Nu=\frac{2}{\ln[R/(R-\delta)]} \tag{20}$$

4. Influence of interfacial waves on heat transfer

Generally speaking, the interfacial wave enhances the heat transfer by three kinds of effects [10,11]: the film thinning effect, the convection effect and the phase-change area enlarging effect. Miyara [10] indicates that, for low Prandtl number of liquid film, $Pr<10$, and low liquid Reynolds number, the convection effect can be neglected. Therefore, we focus here on the other two kinds of effects, as follows:

For every step Δz, following the hypothesis of smooth interface, at first, we determine the in situ film thickness $\delta(z)$ and the average velocity of liquid and vapor phases. The selection of perturbation wavelength λ_E will be introduced later. Utilizing the work analysis method introduced in Part 1, the in situ interfacial boundary conditions can be acquired. The interfacial waves make the film thickness varying periodically in range of the wavelength. At the same time, the waves enlarge the phase-change area. Therefore, the condensation heat transfer coefficient is yielded as:

$$\alpha_{\text{wave}} = \frac{1}{\lambda_E}\int_0^{\lambda_E} \frac{k}{R\ln\frac{R}{R-y(z)}}\,\mathrm{d}s \tag{21}$$

where k is the thermal conductivity of condensate film, $\mathrm{d}s = \sqrt{1+y'^2}\,\mathrm{d}z$ is the elementary area of waving interface. At different time, the condensate film thickness varies as $y(z) = \delta_s(z) + \zeta\cos((2\pi/\lambda_E)z)$. Hence, the Nusselt number with interfacial waves will be

$$Nu_{\text{wave}} = \frac{2\alpha_{\text{wave}}R}{k} \tag{22}$$

5. Results with discussion

Typical numerical analysis are made for illustrating the transport phenomena for saturated vapor flow in vertical mini-tubes with different diameters, and the results are compared to that in a tube of 6 mm i.d. with same inlet vapor Reynolds number $Re_{v0} = 2200$. The typical temperature drop between the vapor and wall surface is taken as $\Delta T = 5$ °C. Three different gravity environments, $g = 0$, 9.81 m/s^2 (vapor flow downward) and $g = -9.81$ m/s^2 (vapor flow upward), are taken into consideration.

The two-phase flow system with smooth phase-change interface in its unsteady equilibrium, and correspondingly, the abilities to produce wave with increasing amplitude are analyzed. Once the interface begins to wave, the suction forces increase at first, due to the narrowing of vapor flow passage, which promotes the waving. Subsequently, the surface tension that restrains the interfacial waves increases gradually. The combined effect of the forces tends to make the wavy interface realizing a somewhat new equilibrium for $E(y) = 0$. Fig. 2 shows the plots of $E(y)$ versus the non-dimensional distance of wave crest, $(y - \delta_s)/R$, from the stable interface for different tube diameters and gravity environments. At the same inlet vapor Reynolds number, Re_{v0}, decreasing tube diameter will increase vapor velocity, and thus enlarge the velocity difference between vapor and condensate film, which results in enhancing the phase-change interface instability due to Bernoulli effect. In addition, it can be deduced from Eq. (5), that, while $[(1/r_{lv,1}) + (1/r_{lv,2})] > 0$, the smaller the tube diameter, the more the obvious effect of capillary force $F_s(\zeta)$ on improving condensate film instability.

It is clear from Fig. 2 that, for the same tube diameters, the film instability will be enhanced by upward vapor flow and microgravity environment as compared with downward vapor flow. This phenomenon can be explained from the enlarging effect of vapor–liquid velocity difference for vapor flow upward, which restrains the improvement of condensate velocity, and hence, enhances film instability due to Bernoulli effect. Also, the thicker condensate film in such environments decreases the interface radius, leads to more obvious effect of capillary force, $F_s(\zeta)$, on improving condensate film instability. However, it would be obvious that, decreasing the tube diameter will weaken the effect of gravity, and therefore, as illustrated in Fig. 2, the difference in film instability due to different gravity environments should be weakened accordingly in small/mini-diameter tubes.

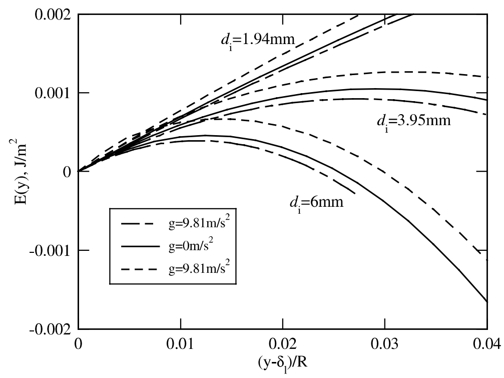

Fig. 2. Influence of tube diameters and gravity with the same vapor quality and wavelength.

The influence of tube wall capillary force on condensate film instability is shown in Fig. 3. Without consideration of capillary force, F_w, on tube wall, the energy involved in displacing wave crest can be always positive and increased with increasing the non-dimensional distance of wave crest, which means that the wave amplitude can continue to grow up until a complete bridging is formed. If the surface tension on tube wall is taken into consideration, $F_w \neq 0$, the energy $E(y)$ will

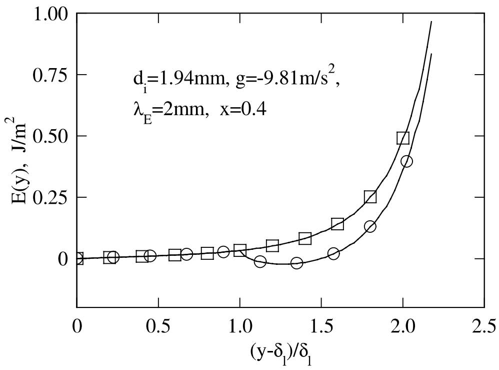

Fig. 3. Influence of tube wall capillary force (□: without consideration of tube wall capillary force; ○: with consideration of tube wall capillary force).

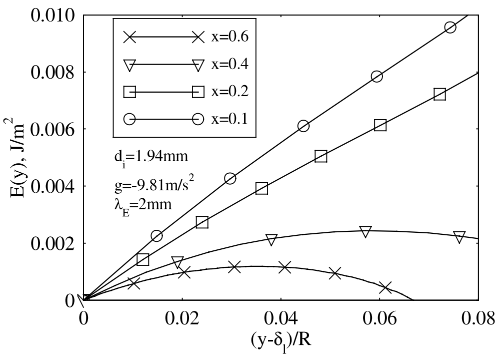

Fig. 4. Energy involved in displacing the wave crest for different vapor qualities.

decrease sharply while the wave spreads to the tube wall, i.e. $(y-\delta)/\delta = 1$, and hence, the condensate film is hard to be broken due to the possible action of adhesion.

Fig. 4 shows the energy involved to increase the amplitude varies for different vapor qualities, x. The interfacial waves become increasingly enhanced with decreasing the vapor quality, x, or with increasing liquid Reynolds number Re_l along the flow path. The thickened condensate film leads to increase the bending effect of liquid–vapor interface along axial direction, so that the influence of capillary force $F_s(\zeta)$ on the interface promotes the interface waving obviously. Besides, from Eq. (5), a thicker liquid film causes the interfacial waves more sensitive to the Bernoulli effect. All these coupled effects would increase the film instability.

Fig. 5 illustrates that the perturbation wavelength has a little complex effects on condensate film instability. As $y < 2\delta$, increasing perturbation wavelength, λ_E, will increase the radius of curvature at wave crest, which may lead to $[(1/r_{lv,1}) + (1/r_{lv,2})] > 0$, and therefore, the capillary force $F_s(\zeta)$ becomes the factor to enhance film instability. However, while the interfacial wave spreads to the tube wall, the increasing wavelength will decrease the intersection degree between condensate film and solid wall, β. According to Eq. (6), the adhesion force, $F_w(\zeta)$, is thus increased, which restricts rising trend of the wave. It is shown in Fig. 5 that, $E(y)$ increases with increasing wavelength as $y < 2\delta$. As $y > 2\delta$, $E(y)$ may decrease sharply while the wavelength increases over a threshold value. This may conclude that the wavy interface has selectivity to perturbation wavelength. Only wavelength in a certain range can lead to breakup of condensate film, which needs to be further analyzed.

In fact, the perturbation wavelength, λ_E, is related to tube diameter and flow conditions during condensation. One can follow Ramkrishna and Pattanayak [8] to obtain

$$\frac{(\bar{u}_v - \bar{u}_l)^2}{I_0'(2\pi r_I/\lambda_E)} I_0(2\pi r_I/\lambda_E)\rho_v = \sigma_{lv} \tag{23}$$

where I_0 is the Bessel function, and $r_I = R - \delta_s$ is the initial position of phase-change interface.

Fig. 6 shows the comparison for Nusselt number of flow film condensation heat transfer with or without the consideration of interfacial waves in a vertical tube of 2.80 mm i.d. Even as the liquid Reynolds number, Re_l, is as low as to 30, the enhancement of heat transfer due to interfacial waves is still to be feasible. To the present analyzed example, in spite of the small liquid Reynolds number, the maximum heat transfer enhancement may be up to 20%. This means in mini-diameter tube, for specified inlet Reynolds number, Re_l, the decrease of tube diameter not only increases the vapor velocity, but also exacerbates the bending of condensed film, and as a result, leads to increase the instability of liquid film, so that the influence of interface waving becomes obvious.

Fig. 7 shows that neglecting the phase-change area enlarging effect due to the interfacial waves hardly has effect on flow condensation heat transfer. The results indicate that, at least in range of low liquid film Reynolds number, the film thinning effect due to the interfacial waves will dominate the heat transfer enhancement.

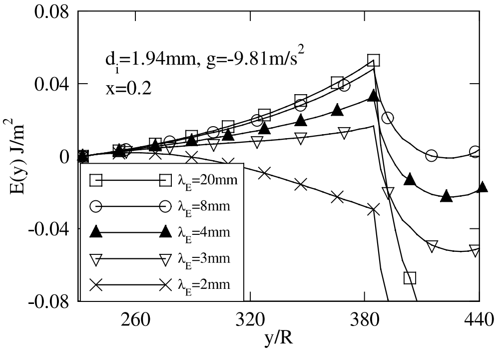

Fig. 5. Influence of the wavelength.

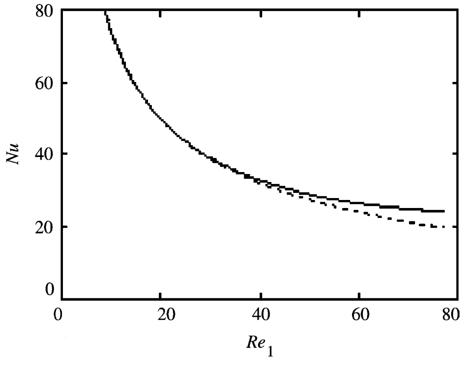

Fig. 6. Influence of interfacial waves ($d = 2.80$ mm) (—) with and (- - -) without consideration of interfacial waves.

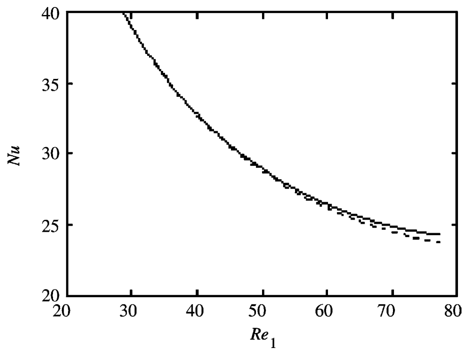

Fig. 7. Influence of area enlarging effect. ($d = 2.80$ mm) (—) with and (- - -) without consideration of interfacial area enlarging effect.

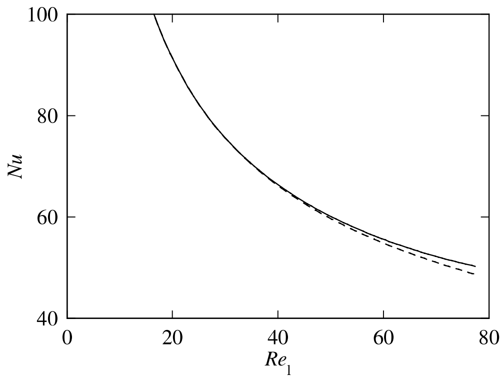

Fig. 8. Influence of interfacial waves ($d = 6$ mm) (—) with and (- - -) without consideration of interfacial waves.

The Nusselt number for flow film condensation in vertical tube of 6 mm i.d. is shown in Fig. 8. As compared to that in tube of 2.80 mm i.d. under same inlet vapor Reynolds number, $Re_{v0} = 2200$, the vapor velocity decreases, and hence, the Bernoulli effect is weakened. Also, the larger the tube diameter, the bending effect of condensate film decreases, and thus reduces the effect of capillary forces on interfacial waves. Therefore, the influence of interfacial waves on flow condensation heat transfer is obviously decreased in 6 mm i.d. tube.

6. Conclusions

Work or energy analysis has been adopted to examine the behavior of wavy interface and its influences on heat transfer for flow film condensation in a vertical mini-tube. The results can be concluded as follows:

(1) The decreasing tube diameter, gravity and quality would increase the instability of the film, while the capillary force on tube wall will stabilize the condensate film, the film will become instable only for a certain range of perturbation wavelength.
(2) As tube inside diameter decreased to below about 3 mm, interfacial waves can appear even at very low film Reynolds number, Re_l, even less than 30. More obvious heat transfer enhancement due to the effect of interfacial waving can be obtained in mini-tube than in normal commercial tube.
(3) In mini-diameter tube, the interfacial waves enhance the heat transfer mainly by film thinning effect, the heat transfer enhancement due to the enlarging interfacial area does not play important role.

Acknowledgements

The research project is financially supported by the National Natural Science Foundation of China with grant no. 59995550-3. X.-Z. Du would like to thank Prof. T.S. Zhao of Hong Kong University of Science and Technology for an appointment as a Visiting Scholar during September 2002 to August 2003.

References

[1] W. Nusselt, Die Oberflächenkondensation des Wasserdampfes, VDI 60 (1916) 541–546.
[2] J.W. Rose, Condensation heat transfer fundamentals, Trans. IchemE 76 (1998) 143–152.
[3] F.P. Incropera, D.P. Dewitt, Fundamentals of Heat and Mass Transfer, John Wiley & Sons Inc., 1985.
[4] W.M. Rohsenow, Film condensation, Appl. Mech. Rev. 23 (1970) 487–496.
[5] B.X. Wang, X.Z. Du, Condensation on the outside surface of a small/mini-diameter tube for vapor flowing through a horizontal annulus surround by an adiabatic concentric tube, Int. J. Heat Mass Transfer 43 (2000) 1391–1398.
[6] B.X. Wang, X.Z. Du, Study on laminar film-wise condensation for vapor flow in an inclined small/mini-diameter tube, Int. J. Heat Mass Transfer 43 (2000) 1859–1868.
[7] B.X. Wang, X.Z. Du, The effect of surface tension on flow condensation in vertical small-diameter tube, Prog. Nature Sci. 10 (2000) 371–378.
[8] D. Ramkrishna, S. Pattanayak, Detection and analysis of transition from annular to intermittent flow in vertical tubes, Can. J. Chem. Eng. 74 (1996) 49–57.
[9] W.H. Henstock, T.J. Hodgson, The interfacial drag and height of the wall layer in annular flows, AIChE J. 22 (1976) 990–1000.
[10] A. Miyara, Numerical analysis on heat transfer of falling liquid films with interfacial waves, in: J.S. Lee, Kyongju (Ed.), Heat Transfer 1998, Proceedings of 11th IHTC, vol. 2, pp. 57–62.
[11] S. Jayanti, G.F. Hewitt, Hydrodynamics and heat transfer of wavy thin film flow, Int. J. Heat Mass Transfer 40 (1997) 179–190.